electronics

MDPI

Article

IO-Link Wireless Sensitivity Testing Methods in Reverberation Chambers

Christoph Cammin [1,*], Dmytro Krush [2], Dirk Krueger [2] and Gerd Scholl [1,*]

1 Electrical Measurement Engineering, Helmut-Schmidt-University, University of the Federal Armed Forces Hamburg, Holstenhofweg 85, 22043 Hamburg, Germany
2 KUNBUS GmbH, Heerweg 15c, 73770 Denkendorf, Germany
* Correspondence: christoph.cammin@hsu-hh.de (C.C); scholl@hsu-hh.de (G.S.); Tel.: +49-40-6541-3354 (C.C.)

Abstract: Communication reliability is a challenging requirement, which implies the need for over-the-air (OTA) testing. Reverberation chambers (RCs) are widely used for OTA tests in various fields. Due to their properties, such as inherent radio channel emulation or the arbitrary orientation of the equipment under test (EUT) in the test volume, they can be used as advantageous test environments for wireless products in the field of industrial manufacturing automation, such as for the IO-Link Wireless (IOLW) standard. In this paper, the different OTA sensitivity test procedures total isotropic sensitivity (TIS), average fading sensitivity (AFS) and mean channel packet error (MCPE) method, which is based on the fundamental channel model of the wireless standard, are described and evaluated in various variants. A core aspect of the proposal is the impact of the possible use of frequency hopping of the wireless equipment under test. The respective advantages and disadvantages are shown. Overall, TIS proves to be a suitable alternative for IOLW OTA sensitivity testing.

Keywords: reverberation chamber; over-the-air testing; OTA; IO-Link Wireless; sensitivity measurement

check for updates

Citation: Cammin, C.; Krush, D.; Krueger, D.; Scholl, G. IO-Link Wireless Sensitivity Testing Methods in Reverberation Chambers. *Electronics* **2022**, *11*, 2775. https://doi.org/10.3390/electronics11172775

Academic Editors: Gabriele Gradoni, Valter Mariani Primiani and Xiaoming Chen

Received: 29 July 2022
Accepted: 30 August 2022
Published: 3 September 2022

1. Introduction

Recently, the need for wireless communication solutions for industrial applications has grown in order to implement flexible manufacturing concepts, such as in the context of Industry 4.0 or Industrial Internet of Things (IIoT). Generally, industrial wireless automation is divided into different domains, such as, for example, process automation, factory automation (FA), logistics, and building automation, each with particular requirements, as described in [1]. A key requirement is always high reliability, which makes testing necessary. In the last years, reverberation chambers (RCs) could be established as test environments for electromagnetic compatibility (EMC) testing with a corresponding standard IEC 61000-4-21 [2] or for antenna measurements [3–5] or over-the-air (OTA) evaluation of wireless devices with integrated antennas [6–9]. In [6], the general use of RCs for wireless device tests was proposed and in [7], different methods for sensitivity measurements were suggested. More than a decade later, [8,10,11] present comprehensive overviews of RC measurements, and finally [9] describes an OTA performance evaluation test plan for large-form-factor devices.

In general, RCs have some characteristics that are beneficial for wireless device testing: RCs consist of an electromagnetically shielded volume, so inside the chamber, interferers are highly damped and are thus negligible, typically even for sensitivity measurements. In addition to an equipment under test (EUT) and at least one antenna for field excitation, there is a mode stirrer, typically made of conductive material, which is rotated or moved in the chamber in a defined manner. Often, several mechanical mode stirrers are combined with a turntable for the EUT and several switchable antennas. Single measurements were performed over a cycle of different mode stirrer conditions or combinations of them. Within the test volume of an ideal RC, the field distribution is quasi-homogeneous and quasi-isotropic with constant mean values, independent of the position of the EUT [8,10,11]. RCs provide an inherent Rayleigh/Rician fading environment [6,12,13], which can often be seen as the worst-case scenario [14–16]. In many conditions, an additional external channel emulator is not necessary [10,12,17,18]. The power delay profile (PDP), or its essential inverse, the coherence bandwidth (CBW), respectively, are tuneable in wide ranges to emulate a realistic environment [12,18–20]. Compared to anechoic chambers (ACs), costly linings with radio frequency (RF) absorbers are largely eliminated, and RCs can be built much more compactly at given wavelengths, resulting in further cost advantages. Overall, RCs thus represent practical and cost-effective test environments. The technical and economical advantages are essential for lower-volume wireless applications to make testing feasible at all. However, various measurement methods exist, such as for determining the sensitivity in a RC (e.g., [7]). In addition, there are variations or detailed adaptations of these methods that must fit to the EUT and its radio standard. The consideration of the respective measurement uncertainties represents a further, important aspect in the selection of an appropriate measurement method. For the estimation of the measurement uncertainty of the RC, numerous publications exist, such as [21,22].

This paper describes the investigation of different measurement methods for the sensitivity evaluation of products for the standard IO-Link Wireless (IOLW) intended for FA. These experiments are also used to investigate corresponding OTA test methods with respect to a test specification that is currently being developed. Nevertheless, the investigations and results can also be applied to other wireless standards with similar characteristics.

The novelty of this work comprises the following:

- A study on the impact of a frequency hopping mechanism on OTA sensitivity measurements compared to measurements at a single frequency in a RC, as IOLW utilizes frequency hopping in normal operation;
- The first—to the author's knowledge—scientific publication on IOLW OTA sensitivity tests;
- A comparison of a total of three different OTA sensitivity measurement methods, additionally with variations.

An introduction to IOLW is described in Section 2. This includes an estimation of the reliability of the IOLW communication, which results in constraints for the following considerations. In Section 3, different methods for sensitivity measurement are presented. A setup to perform and evaluate the different measurement methods is depicted in Section 4. Results are presented in Section 5, and finally a conclusion is given in Section 7.

2. IO-Link Wireless in Factory Automation

Typically, factory environments are subdivided into adjacent 10 m by 10 m manufacturing cells. In most cases, a manufacturing cell consists of a single machine, which performs manufacturing steps. Usually, manufacturing cells have up to about 100 sensors and actuators, which are typically to be operated with a residual communication error probability of $\leq 10^{-9}$ [23]. There is a demand for wireless standards for FA in order to achieve a higher flexibility and to allow an easier retrofit of existing plants.

IO-Link Wireless (IOLW) [24,25] was developed to meet the specific requirements of FA. IOLW is an extension to the industry proven wired IO-Link [26], also standardized as IEC 61131-9 [27]. In a star-shaped topology, a wireless master (W-Master) acts as a base station for wireless devices (W-Devices), i.e., sensors or actuators [28]. Wireless bridges allow to retrofit existing wired IO-Link sensors (e.g., [25,29]). Currently, the international standardization of IOLW is in progress in the IEC as "Industrial networks—Single-drop digital communication interface—Part 3: Wireless extensions, SDCI-W", prospective as IEC 61139-3 [30], and an according test specification is under development, too. The authors are involved in the standardization, and this work is also intended to provide a supporting contribution to the emerging test specification.

The physical layer of IOLW is based on bluetooth low energy (BLE). Thus, the 2.4 GHz band is used with GFSK modulation at 1 Mbit/s on-air bit-rate, resulting in about 1.1 MHz occupied channel bandwidth (OCBW) [24,25]. Up to about 80 frequency channels can be used throughout the whole band. Thereby, a frequency hopping algorithm called HT01 is implemented to mitigate the fading effects and to improve the coexistence behavior [24,25,28]. Furthermore, a blocklisting mechanism allows to omit distinct frequency channels for further coexistence improvement [28,31].

A combined frequency/time division multiple access (F/TDMA) scheme is used for media access. A W-Master supports up to five tracks, which are operated in parallel, i.e., in FDMA. A single track can support up to eight slots with different W-Devices. Thus, a W-Master is able to serve up to 40 W-Devices. Furthermore, up to 3 W-Masters can be operated in close neighborhood, allowing to serve up to 120 W-Devices [24,25,28] in total.

The cycle duration is typically 5 ms. Thereby, the cycle is subdivided into three sub-cycles with a duration of 1.664 ms, each, in which one data exchange between a W-Master and W-Devices takes place. After each sub-cycle, a frequency hopping takes place, whereby the next packet (or a repetition of the previous one) is transmitted outside the typical coherence bandwidth (CBW) of wireless channels in industrial manufacturing environments [28]. In addition, the sub-cycle duration is shorter than the typical coherence time so that the repetitions can be seen mostly as statistically independent trials [15,24,25,28,32]. Most commercial W-Masters are based on a modular architecture, meaning that each track is served by distinct transceiver chips or modules [15]. As a result, the system can be treated as a SISO (single input single output) system per track.

2.1. IO-Link Wireless Reliability Estimation

Reliability is a key requirement on industrial wireless communication systems. Thus, IOLW was designed to ensure a well-defined maximum latency time at a high reliability, for which an estimation is presented in the following. Typically, the sensitivity of a BLE or IOLW chips is defined as the minimum required input power to achieve a bit error probability (BEP) of 10^{-3} (without any interference). This sensitivity level is usually in the order of -94 dBm–-97 dBm for actual transceiver chips (e.g., [24,25,32]). Furthermore, the BEP decreases almost exponentially for receive power levels above the sensitivity level, until a certain residual limit. The packet error probability (PEP) can be obtained from the BEP according to [33] by

$$\mathrm{PEP} = 1 - (1 - \mathrm{BEP})^{n_{Bits}}, \tag{1}$$

where n_{Bits} is the number of bits of the transmitted packet.

IOLW packets consists of 96, 200 or 416 bits [24,25], resulting at the sensitivity level in a PEP ≈ 0.3 for the longest packets. In general, communication reliability is related to the PEP. As presented in [32,34], without interference, the weighted PEP in a fading wireless channel can be calculated as follows:

$$\mathrm{PEP}_{\text{weighted, channel}} = \int_0^\infty pdf_{\text{channel}}(r) \cdot \mathrm{PEP}(r) \cdot dr, \tag{2}$$

where $pdf_{\text{channel}}(r)$ is the probability density function of a wireless channel for a certain power level r, and $\mathrm{PEP}(r)$ is the corresponding packet error probability for the corresponding power level r.

For the reliability estimation of IOLW, a simplified wireless channel model is suggested ([25] Annex K). This wireless channel model consists of two parts, the Friis free-space model for the path loss and the Rayleigh channel to model the small-scale fading.

2.1.1. Free-Space Path Loss (Friis)

Originally, the Friis transmission formula was derived to calculate the path loss in free-space conditions [35]. However, the model is also commonly used to estimate the average receiving power, even in more realistic multi-path environments [14]. Therefore, sometimes the original formula is modified and the exponent 2 is replaced by a path loss factor, which represents average (additional) attenuation in different environments and lies typically between about 2 (free environment) to about 4 (heavily damping environment) [14,36,37]. However, in the IOLW reliability estimation ([25], Annex K), the exponent of 2 is used, resulting in

$$P_{RX} = P_{TX} \cdot G_{RX} \cdot G_{TX} \cdot \left(\frac{\lambda}{4\pi R}\right)^2. \tag{3}$$

Here, P_{RX} and P_{TX} represent the received and the transmitted power in watts, and G_{RX}, G_{TX} represent the (dimensionless) antenna gains of the receiving and the transmitting antennas, respectively. The corresponding wavelength is given by λ, and the distance between the transmitter and the receiver is given by R, both in meters.

2.1.2. Rayleigh Channel

The Rayleigh channel is a common model for small-scale fading, especially for non line of sight (NLOS) wireless channels with severe multi-path propagation. Furthermore, the Rayleigh channel model can often be seen as worst-case scenario [6,14–16]. The probability density function for the receiving signal amplitude is given in [14] as

$$pdf_{\text{Rayleigh}}(s) = \frac{s}{\sigma^2} \cdot \exp\left(-\frac{s^2}{2\sigma^2}\right), \tag{4}$$

where s represents the signal amplitude and σ represents the mode. The corresponding cumulative distribution function is given in [14] as

$$cdf_{\text{Rayleigh}}(s) = 1 - \exp\left(-\frac{s^2}{2\sigma^2}\right) \approx \frac{s^2}{2\sigma^2}, \tag{5}$$

where the approximation holds for $0 < s << \sigma$. With the mean receive signal power $\overline{s^2} = 2\sigma^2$, this model results in the following probability of fading, shown in Table 1.

Table 1. Probability of fading in a Rayleigh channel.

Fading Dip Below	Probability
−10 dB	0.1 (=10%)
−20 dB	0.01 (=1%)
−30 dB	0.001 (=0.1%)

2.1.3. Regulatory Requirements

As one regulatory requirement on IOLW, the final product shall not exceed a total transmitter output power of +10 dBm equivalent isotropic radiated power (EIRP) [38]. Thus, an IOLW W-Master, which serves one track, is allowed to transmit with up to +10 dBm EIRP (peak), but a multi-track W-Master has to share the maximum allowed power over its tracks, i.e., a five-track W-Master can transmit with +3 dBm per track on average. Taking this requirement into account, using Equation (3) with a wavelength $\lambda \approx 0.12$ m and assuming antennas with 0 dBi gain, on both, transmitter and receiver, results in 60 dB path loss for $R = 10$ m and 66 dB path loss for $R = 20$ m. With the maximum allowed transmitter output power, this results in an average receive power of ≤−56 dBm for a one-track W-Master at $R = 20$ m and in an average receive power of ≤−57 dBm for a multi-track W-Master at $R = 10$ m range. Assuming a margin of about 6–8 dB for limited antenna efficiency, mismatch, attenuation of matching circuits, etc., an average receive power in the order of −64 dBm (average over all relevant frequency channels) is taken for the IOLW system design.

Combining the Rayleigh channel with the path loss model and the regulatory requirement, the integral in Equation (2) can be solved, generally. However, this requires a continuous knowledge of the PEP as a function of the receive power. If the PEP as a function of the receive power is known in steps (e.g., by stepwise measurements), the integration can be approximated by stepwise summation. With a sensitivity level (i.e., BEP $= 10^{-3} \rightarrow$ PEP ≈ 0.3) at -94 dBm, the following Table 2 can be used as an approximation.

Table 2. Stepwise approximation of BEP and PEP for IOLW reliability estimation, based on ([25] Annex K).

Probability (Fading Dip below Mean Receive Power)	Receive Power	BEP	PEP
$p(\leq 35\,\text{dB}) \approx 0.0003$	$P_{RX} \leq -99\,\text{dBm}$	≈ 0.1	≈ 1
$p(\leq 30\,\text{dB}) \approx 0.001$	$P_{RX} \leq -94\,\text{dBm}$	$\approx 1 \cdot 10^{-3}$	$\approx 3 \cdot 10^{-1}$
$p(\leq 25\,\text{dB}) \approx 0.003$	$P_{RX} \leq -89\,\text{dBm}$	$\approx 2 \cdot 10^{-5}$	$\approx 8 \cdot 10^{-3}$
$p(\leq 20\,\text{db}) \approx 0.01$	$P_{RX} \leq -84\,\text{dBm}$	$\approx 7 \cdot 10^{-7}$	$\approx 3 \cdot 10^{-4}$
$p(\leq 15\,\text{dB}) \approx 0.03$	$P_{RX} \leq -79\,\text{dBm}$	$\approx 3 \cdot 10^{-8}$	$\approx 1 \cdot 10^{-5}$
$p(\leq 10\,\text{dB}) \approx 0.1$	$P_{RX} \leq -74\,\text{dBm}$	$\approx 1 \cdot 10^{-9}$	$\approx 4 \cdot 10^{-7}$
$p(\text{less than } 10\,\text{dB}) \approx 0.9$	$P_{RX} \geq -74\,\text{dBm}$	$\leq 1 \cdot 10^{-9}$	$\leq 4 \cdot 10^{-7}$

Applying the approximation of Table 2 results in $\text{PEP}_{\text{weighted}} \approx 0.7 \cdot 10^{-3}$ for one transmission trial in single direction without interference. Using this intermediate result and the previously stated assumption that the repetitions in different sub-cycles are statistically independent (outside the CBW, etc.), the residual failure probability (RFP), for example, with 3 attempts (i.e., 2 retries), can be calculated for a single direction transmission as

$$\text{RFP} = \left(\text{PEP}_{\text{weighted}}\right)^3 \approx \left(0.7 \cdot 10^{-3}\right)^3 \approx 3.4 \cdot 10^{-10} < 10^{-9}. \quad (6)$$

2.2. IOLW Testing

In order to ensure that the assumptions, especially regarding the link budget, can basically be met, measurements and tests are of great importance. The main approaches for IOLW testing are as follows: self-testing and self-declaration by manufacturers is an industrial requirement on IOLW for cost-effective testing. Furthermore, the tests should be designed mostly as end-to-end tests, allowing normal operation mode, without designing specific test modes. As no commercial base-station emulators or IOLW specific test hardware is commercially available yet, protocol-related tests shall be performed, using well-characterized "Golden W-Masters" and "Golden W-Devices" as test companions [15,28]. OTA tests are necessary for modules and products with integrated antennas. In particular, W-Devices will be highly integrated with small antennas. Mostly, performance indicators obtained over the full sphere are useful, because the position and orientation of small, integrated W-Devices will be related to the final application.

Due to the beneficial characteristics stated in Section 1, RCs are also suggested for IOLW sensitivity testing [15,28,39]. However, IOLW product manufacturers require, in principle, test procedures for both ACs and RCs. Sensitivity tests (of products with integrated antennas) represent a special challenge, which will be considered in more detail below.

3. Sensitivity Measurement Methods

As indicated before in Section 2.1, the transmitter output power and the receiver sensitivity are important figures of merit. However, the focus of this paper is on sensitivity measurements only. Different methods to measure the receiver sensitivity are currently under discussion for IOLW products with an integrated antenna:

- Mean channel packet error (MCPE).
- Total isotropic sensitivity (TIS).
- Average fading sensitivity (AFS).

Testing parameters, such as the configuration of the RC or exact numbers for the testing level, number of steps, packets, etc., are also not fixed yet. In the following, these three basic methods are briefly presented.

3.1. Mean Channel Packet Error (MCPE)

The approach for the MCPE method in RCs is based on the fact that, as described in Section 2.1, IOLW products are expected to operate with the required reliability at a certain average received power and a Rayleigh channel as the worst-case scenario. The following is assumed here: the mean power level, which refers to the antenna port of a reference antenna (such as a dipole or discone type antenna) is chosen as the average receive power according to the IOLW system design and considering the regulatory requirements as indicated in Section 2.1.3, i.e., $P_{avg.} \approx -58\,\text{dBm}$ with minor deviations due to some margin for an antenna matching network, balun, losses in traces and limited efficiency. Starting from the chosen mean receive power, the probability of fading dips of a certain value can be obtained from the Rayleigh channel theory as described in Section 2.1.2, and in particular in Table 1. With such a RC setup, a receive power of around $-88\,\text{dBm}$ (at a reference antenna) will be achieved with a probability of about 0.001 or 0.1%. Furthermore, it is assumed from the reliability estimation in Section 2.1 that a packet error is tolerable for very low receive power levels (i.e., the designed mean receive power minus the fading margin and with respect to the margin for antenna efficiency). In other words, a PEP ≈ 1 at the designed mean receive power minus the fading margin and with respect to the margin for antenna efficiency would not inhibit the "10^{-9}" goal. In addition, the typical behavior of IOLW (narrowband GFSK) transceivers is that with slightly higher receive power above the sensitivity limit, the BEP and the PEP decrease extremely fast. With less deep fading dips of, for example, not deeper than $-25\,\text{dB}$ to the mean level, the PEP is not significant, and these fading dips have only a minor influence on the overall IOLW system robustness, as outlined in Table 2. Simplified, the dependence of the PEP on the received power can be interpreted as an (inverted) step function: below the sensitivity limit, the PEP is approximately one, and for received power above the sensitivity limit, the PEP is negligible low.

This results in the following measurement procedure: Firstly, the transmit power of the test companion (i.e., the transmitter which generates the on air packets) is set to a level which represents a mean received power at the EUT of $-58\,\text{dBm}$ (previously characterized using a reference antenna) for a full mode stirring cycle. In order to achieve reproducible testing, the configuration of the RC, such as its loading with RF absorbers and the stirring sequence, is kept constant for the actual test of the EUT. Furthermore, it is suggested that 100 packets (at least) per utilized frequency and each mode-stirrer (combination) step are sent to the EUT. Therefore, the packets shall have maximum packet length.

The EUT shall acknowledge the correct reception of every packet. Therefore, the EUT transmits at maximum power and/or with less attenuation than in the reception direction, i.e., asymmetric testing. The PEP shall be estimated as follows:

$$\text{PEP} \approx \frac{\text{Number of packets correctly received (acknowledged) by EUT}}{\text{Number of packets send to EUT}}. \tag{7}$$

However, it is also possible to estimate PEP by the number of correctly received packets only, if the number of packets send to the EUT is known a priori. The test criteria are related to the average PEP (over both frequencies and stirrer steps). The limit to pass this test shall be in the order of

$$\text{PEP}_{average} \leq 10^{-3}. \tag{8}$$

3.2. Total Isotropic Sensitivity (TIS)

Generally, many publications on the total isotropic sensitivity (TIS) method exist, e.g., [7,9,34,40–44]. Furthermore, procedures to measure TIS in an AC exist, e.g., [43].

The TIS procedure consists of the steps outlined in the following: At first, the chamber reference transfer function G_{ref} has to be determined during a reference measurement as

$$G_{ref}(f) = \frac{1}{MN} \sum_{n=1}^{N} \sum_{m=1}^{M} \frac{|S_{21,m,n}(f)|^2}{e_{meas}(f)\eta_{meas}(f) \cdot e_{ref}(f)\eta_{ref}(f)}. \tag{9}$$

Thereby, N and M correspond to the total number of individual fixed measurement antennas n in the chamber and mode stirrer steps m and $S_{21,m,n}$ to the respective scattering parameters, which can be measured with a vector network analyzer (VNA). $e_{meas}(f)$ and $e_{ref}(f)$ are the mismatches of the reference and measurement antenna of frequency f, and $\eta_{meas}(f)$ and $\eta_{ref}(f)$ are the antenna efficiencies over frequency, respectively. For the actual test of the EUT, the configuration of the RC has to be kept constant.

Utilizing stepped mode operation of the RC, the "sensitivity limit", related to a certain PEP (i.e., PEP = 0.3) is searched for: during each mode-stirrer step combination, the output power of the test companion (i.e, of a W-Master if a W-Device is the EUT) is lowered such that the EUT receiver achieves a certain PEP of, for example, PEP = 0.3. The estimated receiving power, i.e., the output power of the test companion achieving that certain PEP value minus the according chamber reference transfer function, is stored. Finally, the (harmonic) mean value of the stored (e.g., 150) estimated receiving power levels is calculated and referred to the TIS value as

$$P_{TIS} = G_{ref}(f) \cdot e_{meas}(f)\eta_{meas}(f) \cdot L(f) \cdot \left(\frac{1}{MN} \sum_{n=1}^{N} \sum_{m=1}^{M} \frac{1}{P_{TX,m,n}(f)} \right)^{-1}. \tag{10}$$

Thereby, $L(f)$ corresponds to the loss of cables, connectors, etc., over frequency f. $P_{TX,m,n}(f)$ is the transmitter output power of the test companion for fixed antenna n and mode stirrer step m over frequency. A TIS value of $P_{TIS} \leq -90$ dBm over all frequencies can be suggested for IOLW, but is not fixed yet.

The TIS procedure has the following advantages: It is well described in the literature as producing results, which are comparable to measurements in an AC. By principle, the TIS value is related to wired sensitivity and taking the antenna efficiency into consideration. However, the TIS procedure is a bit more complex compared to the other candidates, as it requires an adjustable output power of the companion per step.

3.3. Average Fading Sensitivity (AFS)

The procedure to measure the average fading sensitivity (AFS) is described, e.g., in [7,34,44]. In contrast to the previously proposed OTA sensitivity test methods, which utilize stepped mode operation of the RC, the AFS procedure is performed during the continuously moving mode stirrer operation.

The detailed procedure to measure the AFS is as follows: At first, the chamber reference transfer function is obtained, as in Equation (9) but with the difference that the $S_{21,m,n}(f)$-samples are not measured during the standstill of the mode stirrers and instead during their movement. This means that the mode stirrers continue to move during the frequency sweep of the VNA.

During the test with the EUT, the input power of the RC provided by the communication companion is left constant for a full mode stirring cycle, and the average PEP is measured while the mode stirrers are continuously moving. The full mode stirring cycles are repeated to search for a certain average PEP (e.g., $\text{PEP}_{\text{AFS}} = 0.3$). Finally, the corresponding (constant) input power (taking into account the reference transfer function), which leads to that certain average PEP (e.g., $\text{PEP}_{\text{AFS}} = 0.3$) is defined as the AFS. Additionally, here, a limit value is not fixed but is assumed to be around -90 dBm over all relevant frequencies.

In particular, the continuous operation has side effects: Generally, the test duration can be reduced, whereby in general the statistical parameters, such as mean receive power, fading, etc., are identical. However, the accuracy may decrease: the repeatability is also limited in such way that two measured sequences with the same configuration lack correlation in terms of sample-by-sample comparison at continuous operation. Thus, the sequences of measured $S_{21,m,n}$-samples obtained in two measurement series are typically significantly less strongly correlated than if the measurement series were obtained in each case with stepwise operation of the mode stirrers. Even small fluctuations in the speed of movement of the mechanical mode stirrers and a temporal jitter in the measurement or sweep duration of the VNA or the temporal pauses between the measurements or sweeps lead to a loss of synchronicity between motion and the measurement/sweep as the duration of the measurement sequence increases. Hence, the samples originating from different repetitions of the measurement procedure are ultimately captured at slightly different states in the RC. Furthermore, depending on the chamber and the velocity of the mode stirrer(s) in continuous operation, Doppler spread may become relevant.

3.4. Comparison of Methods

Table 3 shows a summary comparison of the three previously mentioned methods and their characteristics.

Table 3. Comparison of the sensitivity test methods, as described in this section.

	MCPE	**TIS**	**AFS**
RC mode	stepped	stepped	continuous
Procedure	Measure PEP at every RC step at constant power, calculate $\mathrm{PEP}_{\mathrm{average}}$	Search for $\mathrm{PEP} = 0.3$ at every RC step, harm. mean of req. power	Perform full stirring sequence at const. power, repeat until $\mathrm{PEP}_{\mathrm{AFS}} = 0.3$
Prospective limit	$\mathrm{PEP}_{\mathrm{average}} \leq 10^{-3}$ at $-58\,\mathrm{dBm}$	$P_{\mathrm{TIS}} \leq -90, \mathrm{dBm}$	$P_{\mathrm{AFS}} \leq -90, \mathrm{dBm}$
Note	related to "natural" operation of IOLW	well researched; comparable to AC measurements	fast and simple

For these three basic methods, there are different variants or modification possibilities, which are briefly described in the following.

3.5. Modifications and Variations

Possible modifications concern the possible use of the frequency hopping method during testing or essentially aim to shorten the measurement duration.

3.5.1. Single Frequency Operation vs. Using Hopping Scheme HT01

In principle, there is the possibility to perform the test methods either at a single frequency or successively at a sequence of frequencies, such as low, medium and high frequency in the 2.4 GHz band or even at all frequencies used by the radio system. If performed consecutively at different frequencies, the mode stirrer sequence in the RC would be repeated accordingly. For the real use of IOLW, however, a frequency hopping procedure over a maximal range of frequencies is intended, as described in Section 2. This leads to the questions of whether both approaches (i.e., measurement at one frequency at a time or by means of an activated frequency hopping) lead to the same results and which approach is more beneficial.

3.5.2. MCPE: Modified Limits

As a modification to the MCPE method, it would be possible to measure the PEP at a lower average received power, at which the average PEP will be higher as specified in Table 3. The advantage of this variant is that the higher permissible average PEP means that fewer packets have to be transmitted overall and thus the measurement duration can be reduced significantly. In particular, it could be useful to measure the average PEP instead of at approximately −58 dBm with 10 dB or 20 dB lower mean received power. Under the highly simplified assumption of the receiver model with the (inverted) step function and instead of measuring the PEP at about −58 dBm and taking $\mathrm{PEP}_{\mathrm{average}} = 10^{-3}$, the corresponding PEP limit is $\mathrm{PEP}_{\mathrm{average},-10\,\mathrm{dB}} = 10^{-2}$ $\mathrm{PEP}_{\mathrm{average},-20\,\mathrm{dB}} = 10^{-1}$, respectively.

3.5.3. MCPE: Continuous Mode Stirrer Movement

Instead of performing the MCPE method as described in Section 3.1 with stepped mode operation, this method can also be modified to measure the average PEP with continuous mode stirrer operation. If this modification is further combined with a reduction in the mean received power and a corresponding adjustment of the PEP limit (as described in the previous section), the procedure is almost the same as the AFS measurement procedure.

3.5.4. TIS: Use of Receiver Information

Some special variants of the TIS procedure, typically focusing on faster testing, also exist. Brand names of these modified variants are "Fast TIS" or "Q-TIS (Quick-TIS)". Often, these improved methods require additional information, such as received signal strength indication (RSSI) values of the receiver under test, i.e., of the EUT, as described, for example, in [45] within an AC. However, these variations will not be considered in detail in the following.

3.5.5. Asymmetric Testing

In general, for all methods and variations, sensitivity testing shall be performed as asymmetric testing. Asymmetric testing in the context of sensitivity means that different power levels toward the EUT and from the EUT are used. The power values should be set in such a way that the EUT transmits with maximum power and the power received at the counterpart (which was emitted by the EUT) is significantly larger, at least on average, than the power arriving at the EUT. As a result of this asymmetry in the receive power levels (i.e., asymmetrical testing), it can be assumed that the (bit/packet) error probability on the way from the EUT to the test equipment is significantly lower than in the other direction. Thus, it can be assumed in good approximation that this return path is error-free, and the measured PEP is caused by the receiving performance of the EUT only.

4. Measurement Setup

As a prerequisite for sensitivity testing in a RC, a suitable configuration of a RC in terms of its loading with RF absorptive material is essential, as described in the following.

4.1. RC Loading

The power delay profile (PDP) in a RC is exponentially decreasing, generally [6,12,18,46,47]. As a figure of merit to describe the PDP, the RMS delay spread τ_{RMS} is commonly used, which can be obtained according to [10,14,39] by calculating

$$\tau_{RMS} = \sqrt{\overline{\tau^2} - (\overline{\tau})^2} \tag{11}$$

with

$$\overline{\tau} = \frac{\sum_k a_k^2 \tau_k}{\sum_k a_k^2} = \frac{\sum_k P(\tau_k)\tau_k}{\sum_k P(\tau_k)} \tag{12}$$

and

$$\overline{\tau^2} = \frac{\sum_k a_k^2 \tau_k^2}{\sum_k a_k^2} = \frac{\sum_k P(\tau_k)\tau_k^2}{\sum_k P(\tau_k)}. \tag{13}$$

The power of the k-th multi-path component that arrives with the delay τ_k is denoted by $P(\tau_k)$. Employing the inverse fast Fourier transform $IFFT_f$ of S_{21}-measurements over frequency f,

$$P(\tau_k) = \overline{\left|IFFT_f(S_{21})\right|^2} \quad (14)$$

can be calculated, whereby the mean of $\left|IFFT_f(S_{21})\right|^2$ over all combinations of stirrer positions (i.e., over M and N) is taken. Several papers discussed the effects of loading a RC with RF absorbing material, e.g., in [6,12,48–50]. Generally, loading leads to a decreased τ_{RMS} of the PDP and an increased CBW of the radio channel within the RC [6,10,12,39,48–50]. The CBW describes the "flatness" of a wireless channel over frequency and is essentially the inverse of the RMS delay spread.

As described, for example, in [8,9,12,17,39], a *too narrow* CBW can cause an increased PEP. Thus, typically, the CBW is increased for sensitivity testing by carefully adding RF absorbers to the RC (i.e., loading the RC) [8,9,12,17]. Depending on the wireless standard (i.e., occupied channel bandwidth (OCBW), modulation scheme, and coding), different CBW or τ_{RMS} have to be adjusted [8,10,21,40,47,51]. For this purpose, the loading of a RC and the resulting RMS delay spread τ_{RMS} or CBW were varied in [39], whereby the EUT and other settings, such as the received power, were kept constant. Thereby, a saturation in the PEP (or link quality) was observed. The loading at which this saturation effect occurs or the τ_{RMS} up to which this effect occurs was recommended as the loading for future tests. For IOLW testing, a RMS delay spread of $\tau_{RMS} = 50\,\text{ns}$ is suggested, according to this previous work [39]. However, this value is not officially fixed for IOLW testing, yet. With a common formula, the corresponding CBW can be calculated according to, for example, [8,19,20] as follows

$$\text{CBW} = \frac{\sqrt{3}}{\pi \cdot \tau_{RMS}} \Rightarrow \frac{\sqrt{3}}{\pi \cdot 50\,\text{ns}} \approx 11\,\text{MHz}. \quad (15)$$

This CBW is significantly larger than the occupied channel bandwidth (OCBW) of IOLW, which is typically about 1.1 MHz. A similar "over flattening" was also report in literature, especially for NB-IoT communication systems [41,51].

4.2. Procedure Evaluating Measurements

Measurements were performed with the same W-Device prototype as EUT to evaluate the different methods. The focus is not on assessing compliance with possible limit values, but rather on gaining experience with the processes and trialing suitable modifications. Figure 1 shows a sketch of the essential measurement setup.

The measurements were performed using the same EUT in a Bluetest RTS60-type chamber [52]. This RC has two planar mode stirrers (wall and ceiling), a turntable for the EUT, and an arrangement of three fixed antennas behind a shielding blade (i.e., $N = 3$ in Equation (9)), whereby the shielding blade shall suppress a direct path. As indicated in Section 4.1, a RC loading with a corresponding RMS delay spread of $\tau_{RMS} = 50\,\text{ns}$ was realized. As a communication companion, the same W-Master prototype was used during all measurements. In order to exclude external interferers, the W-Master prototype was operated in an external shielding enclosure dBsafe RME, which, as well as the RTS60 with the W-Device prototype inside, provide more than 100 dB effective shielding in the relevant frequency range, according to the datasheets [52–54]. Figure 2 shows a photo of the setup inside the RC.

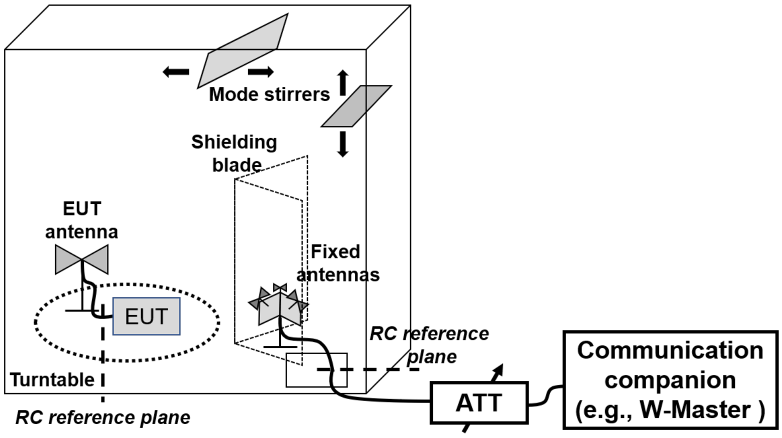

Figure 1. Sketch of the measurement setup.

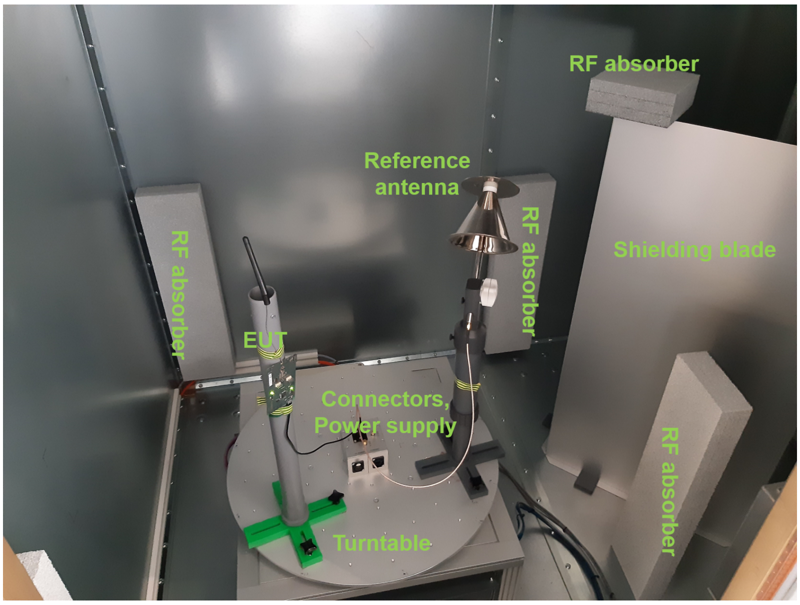

Figure 2. Photo of the measurement setup inside the RC.

To reduce the measuring effort, the methods described above were performed with a selection of variations. In particular, operation frequencies were limited to a selection to either a medium frequency of 2440 MHz (mid), or a set of three frequencies of 2403 MHz (low), 2440 MHz (mid) and 2475 MHz (high), or frequency hopping according to HT01 (in the following referred to as HT01) was chosen, as described in more detail below. For comparability, all methods which are based on stepped mode operation of the stirrers were performed with 150 RC step combinations (i.e., $M = 50$ and $N = 3$ in Equation (9)), each. These were composed of 10 positions of the turntable, combined with 5 positions of the planar mode stirrers on the wall and ceiling (which are moved simultaneously and occupy each of these five positions on their path) and the combination of the 3 fixed antennas.

During continuous mode stirrer operation, the turntable, as well as the mode stirrers on the wall and ceiling, were moved simultaneously. A sequence lasted about 960 s, with the antenna being switched after 320 s in each case. Meanwhile, the PEP was logged about every 90 s. The switching of the antennas during the measurements was realized by relays and was sufficiently fast such that it has no relevant influence on the results.

The MCPE method was evaluated for both, using the mid frequency of 2440 MHz (i.e., mid frequency) and in another measurement series, with frequency hopping over the whole frequency band (i.e., HT01, without blocklisting). In both cases, continuous mode stirring was used in addition to stepped-mode stirring in separate measurement series. In addition, the mean receive power level was reduced in further measurement series. Table 4 lists the evaluated variants of the MCPE method.

Table 4. Evaluated variants of the MCPE method.

RC Mode	Freq.	Set $P_{avg.}$	Note
stepped	HT01	−58 dBm	"original" method
stepped	HT01	−68 dBm	
stepped	HT01	−78 dBm	
stepped	HT01	−88 dBm	
stepped	2440 MHz	−58 dBm	
stepped	2440 MHz	−68 dBm	
stepped	2440 MHz	−78 dBm	
stepped	2440 MHz	−88 dBm	
continuous	HT01	−58 dBm	
continuous	HT01	−68 dBm	
continuous	HT01	−78 dBm	
continuous	HT01	−88 dBm	
continuous	2440 MHz	−58 dBm	
continuous	2440 MHz	−68 dBm	
continuous	2440 MHz	−78 dBm	
continuous	2440 MHz	−88 dBm	

The TIS procedure was performed at 2403 MHz, 2440 MHz, and 2475 MHz, i.e., low, mid and high frequencies, and in another measurement series with HT01 switched on (without blocklisting), respectively.

The AFS procedure can (almost always) only be performed over all relevant frequencies and not over just a single frequency or a single (narrowband) channel since a fading dip with longer duration at that certain frequency causes not only packet errors, but also communication interruptions (i.e., outages) within the IOLW system. (In real-world applications, this is not the case, as an IOLW system has to utilize at least a certain number of frequencies according to the HT01 algorithm such that a packet error on a single frequency can be "healed" by the repetition at another frequency outside the CBW.) Additional variations for the TIS and the AFS procedure were not tested.

5. Results

First, the EUT rod antenna efficiency was determined to be about −1 dB. The antenna efficiency can be assumed to be flat over the complete frequency band. Then, the sensitivity of the EUT was measured with a coaxial cable connection (conducted), in order to determine the reference values. In the following, the results were rounded to integer values. The conducted sensitivity level was reached at about −96 dBm at 2403 MHz, −95 dBm at 2440 MHz and −95 dBm at 2475 MHz. Hence, the frequency response was also reasonably flat. Measurements were carried out according to the different methods MCPE, TIS and AFS.

5.1. MCPE Results

Table 5 presents the results of the MCPE method and its tested variants. The mean and median of the individual PEP measurements (i.e., PEP_{mean} and PEP_{median}, respectively) are given. These were calculated over internally reported PEP measurement values, which were taken for each mode stirrer step with a stepped mode operation of the mode stirrers and over about 90 s with continuous movement of the mode stirrers, respectively.

Using stepped mode operation, the median PEP_{median} was significantly smaller than the PEP_{mean}. This can be related to the fact that there were outliers, i.e., individual mode stirrer combinations, in which a particularly high PEP was achieved. One reason for this may be that the causal deep fading dips are afflicted with outliers, as it was investigated in [55]. Moreover, PEP was relatively similar using the MCPE variants, whether at −58 dBm or −68 dBm mean receive power setting. Thereby, the number of samples in the deep fading area are low, i.e., 0.001 or 0.01 times the number of total samples. Thus, the overall number of measured packets has to be quite large, because only 0.001 of them are in the "interesting" fading deepness, if the simplified "inverse step receiver" is assumed. In addition, the individual PEP values fluctuate with these settings, and the requested low number for the PEP requires a large number of packets to be tested, which is related to an inefficient large measurement duration.

Table 5. Results of the MCPE method.

RC Mode	Freq.	Set $P_{avg.}$	$\mathbf{PEP_{mean}}$	$\mathbf{PEP_{median}}$	Note
stepped	HT01	−58 dBm	$2.9 \cdot 10^{-3}$	$8.0 \cdot 10^{-4}$	
stepped	HT01	−68 dBm	$7.5 \cdot 10^{-3}$	$4.7 \cdot 10^{-4}$	
stepped	HT01	−78 dBm	$3.5 \cdot 10^{-2}$	$3.0 \cdot 10^{-2}$	
stepped	HT01	−88 dBm	$2.6 \cdot 10^{-1}$	$2.5 \cdot 10^{-1}$	outages
stepped	2440 MHz	−58 dBm	$5.6 \cdot 10^{-6}$	0	
stepped	2440 MHz	−68 dBm	$8.4 \cdot 10^{-4}$	0	
stepped	2440 MHz	−78 dBm	$8.6 \cdot 10^{-3}$	$1.0 \cdot 10^{-4}$	outages
stepped	2440 MHz	−88 dBm	$8.6 \cdot 10^{-2}$	$8.1 \cdot 10^{-3}$	outages
continuous	HT01	−58 dBm	$2.4 \cdot 10^{-3}$	$2.0 \cdot 10^{-3}$	
continuous	HT01	−68 dBm	$5.6 \cdot 10^{-3}$	$5.3 \cdot 10^{-3}$	
continuous	HT01	−78 dBm	$2.4 \cdot 10^{-2}$	$2.4 \cdot 10^{-2}$	
continuous	HT01	−88 dBm	$1.5 \cdot 10^{-1}$	$1.5 \cdot 10^{-1}$	
continuous	2440 MHz	−58 dBm	$3.1 \cdot 10^{-3}$	$3.4 \cdot 10^{-3}$	
continuous	2440 MHz	−68 dBm	$3.6 \cdot 10^{-3}$	$3.2 \cdot 10^{-3}$	
continuous	2440 MHz	−78 dBm	$9.6 \cdot 10^{-2}$	$4.0 \cdot 10^{-3}$	outages
continuous	2440 MHz	−88 dBm	$8.3 \cdot 10^{-2}$	$1.1 \cdot 10^{-2}$	outages

Outages occurred as expected when using only one frequency and decreased the mean receive power, both with continuous and stepped mode operation of the mode stirrers. With continuous mode stirrer operation using HT01 and reduced mean receive power, the MCPE method is nearly equivalent to the AFS method. However, the results with regard to the occurrence of outages are slightly different, due to the limited repeatability of the exact frequency-selective fading sequence during continuous operation.

5.2. TIS Results

The results for the conducted reference values as well as for the TIS and AFS methods are presented in Table 6. The results of the TIS measurement at the individual frequencies, low, mid and high (i.e., 2403 MHz, 2440 MHz and 2475 MHz, respectively), agree with the results of the conducted measurements by taking into account the EUT rod antenna efficiency. It is noticeable that the TIS measurement with activated frequency hopping (HT01) led to a significantly less favorable value and to a clear difference to the conducted measurement. Therefore, the corresponding TIS measurement was repeated, but led to the same result. The basic difference with active HT01 is that the receiver has to receive the packets on a different frequency in a frequency-selective radio channel, i.e., the internal, controllable amplifier stages must be significantly changed or adapted for each new packet. In contrast, the packets have the same power in the conducted measurements. Additionally, in the TIS measurements at a single frequency, the power of the packets at the receiver is basically constant for a single, quasi-static mode stirrer combination. However, the TIS measurement using HT01 is faster to perform overall than on single frequencies step by step, and also leads to a more realistic result in terms of the behavior of an IOLW system in a real-world application.

Table 6. Results of the TIS and AFS methods and conducted measurements (each rounded to integer values).

Method (Name)	RC Mode	Freq.	Sensitivity	Note
Conducted	-	HT01	−95 dBm	
Conducted	-	2403 MHz	−96 dBm	
Conducted	-	2440 MHz	−95 dBm	
Conducted	-	2474 MHz	−95 dBm	
TIS	stepped	HT01	−89 dBm	
TIS	stepped	HT01	−89 dBm	(measurement repetition)
TIS	stepped	2403 MHz	−94 dBm	
TIS	stepped	2440 MHz	−93 dBm	
TIS	stepped	2475 MHz	−93 dBm	
AFS	continuous	HT01	−89 dBm	with outages (without outages: −86 dBm)

5.3. AFS Results

The AFS method resulted in −89 dBm with an associated $PEP_{AFS} \leq 0.3$, as shown in Table 6. Single outages occurred in the sense that an internal meter reading required for measurement, which is transmitted acyclically, could occasionally not be transmitted. Without outages, the AFS value was −86 dBm. As indicated in Section 4.2 before, due to frequent outages, the AFS method is not useful when using only one single frequency.

6. Measurement Uncertainty Estimation

As outlined in the Introduction, the consideration of the respective measurement uncertainties associated with the measurement methods represents another significant aspect in the choice of a suitable one. In particular, measurement uncertainty estimations for the TIS method are described for instance in [22,56]. The following brief consideration on measurement uncertainty (MU) estimation essentially follows the examples shown therein. Table 7 lists the components which are considered to contribute to the uncertainty estimation for TIS measurements on one single frequency at a time (i.e., without frequency hopping). According to the data sheet [52], the "accuracy" for passive measurements and TIS measurements are considered here as the uncertainty contribution, which already includes the uncertainty due to a lack of spatial uniformity.

For measurements with frequency hopping enabled (i.e., HT01), it is not possible to determine on which frequency a packet error occurred when obtaining the mean packet errors using standard functionalities implemented in IOLW (as required, see Section 2.2). It follows that for the reference transfer function G_{ref} as well as for the output power of the communication companion, the mean values over the frequency can be used. As a first approach in the uncertainty estimation, the frequency response (or even ripple) related to these mean values can be taken into account by a corresponding additional measurement uncertainty component. Assuming that the frequency response (or ripple) is ± 1 dB over frequency and, as a worst case estimation, rectangularly distributed results in an additional uncertainty component of 0.33 dB, according to [57]. This additional component is considered for both the EUT measurement part as well as reference measurement part, which finally results in a total expanded uncertainty of 1.84 dB.

According to [2], the velocities of the mode stirrers during continuous operation should be (chosen) slow such that they have a negligible influence (e.g., with respect to the resulting Doppler shift). As a consequence, it can be assumed in a simplified way that there is no significant difference between measurements in stepped or continuous mode stirrer operation. Basically, it is further assumed that the same uncertainty components influence measurements according to the TIS and the AFS method and that both have a reference measurement part and an EUT measurement part. Thus, the total measurement uncertainty for the AFS method is assumed to be equal to the one of the TIS method with HT01, i.e., a total expanded uncertainty of 1.84 dB.

Table 7. Components for measurement uncertainty estimation for TIS measurements on single frequencies.

Uncertainty Contribution	Std. Unc.	Reference	Note
Contributions in EUT measurement part			
Mismatch (Com. companion—fixed antenna)	<0.01 dB	[56]	see also [22]
Communication companion output level (stability)	0.18 dB	[22]	assumed to be equal
Cable factor: fixed antenna	<0.01 dB	[56]	see also [22]
Insertion loss: fixed antenna cable	<0.01 dB	[9]	see also [22]
Sensitivity search step size	0.29 dB	[56]	step size: 1 dB
Temperature variation	0.14 dB	[22]	assumed to be equal
Miscellaneous uncertainty	0.10 dB	[56]	
RC accuracy, TIS	0.50 dB	[52]	
Frequency resolution	0.05 dB	[22]	assumed to be equal
Contributions in reference measurement part			
Mismatch (VNA—fixed antenna)	<0.01 dB	[56]	see also [22]
Mismatch (VNA—reference antenna)	<0.01 dB	[56]	see also [22]
VNA absolute level/stability	0.30 dB	[22]	assumed to be equal
Insertion loss: cal. ref. antenna cable	<0.01 dB	[9]	see also [22]
Insertion loss: meas. antenna cable	<0.01 dB	[22]	assumed to be equal
RC accuracy, passive	0.30 dB	[52]	
Antenna: radiation efficiency reference antenna	0.29 dB	[56]	
Total expanded uncertainty		1.60 dB	expansion factor: 1.96

The following estimation of the measurement uncertainty for the MCPE method is based on the assumption of the "inverse step receiver" model as well as the properties of the Rayleigh channel.

First, it is considered that the mean radio channel for the MCPE method can be determined with the same uncertainty as the reference transfer function of the TIS method. In [55], the reproducibility of fading dips was examined for this RC with different parameters. The estimated standard deviation of fading dips −10 dB, −20 dB or −30 dB between different measurement series at different positions and orientations in the RC was calculated. For further considerations, the values from ([55] Table 1) with the parameters “300 steps” and a loading that resulted in “50 ns” are assumed to be the closest applicable, even though a different number of mode stirrer step combinations is used here. According to ([55] Table 1), these are estimated standard deviations over the positions/orientations of 0.18 dB for fading dips of −10 dB below the mean, 0.58 dB for fading dips of −20 dB below the mean and 1.83 dB for fading dips of −30 dB below the mean. For the original MCPE method, the mean channel in the RC is set to be about 30 dB above the sensitivity limit. It follows that 1.83 dB is then assumed as an additional component for the measurement uncertainty in the EUT measurement part according to this difference to the limit value. For the variants of the MCPE method with changed average powers in the RC, the further values are assumed accordingly. With the previously stated assumption of negligible effects due to continuous mode stirring, the RC mode is irrelevant for the uncertainty estimation of the MCPE method. Table 8 lists the estimated total expanded measurement uncertainties for the different methods.

Table 8. Overview of estimated, total expanded measurement uncertainties for different sensitivity measurement methods (each includes a coverage factor of 1.96).

Method (Name)	RC Mode	Freq.	estimated MU	Note
TIS	stepped	single freq.	1.60 dB	
TIS	stepped	HT01	1.84 dB	
AFS	continuous	HT01	1.84 dB	
MCPE	*(irrelevant)*	single freq.	1.60 dB	$P_{avg.}$ at sensitivity limit
MCPE	*(irrelevant)*	single freq.	1.63 dB	$P_{avg.}$ 10 dB above limit
MCPE	*(irrelevant)*	single freq.	1.96 dB	$P_{avg.}$ 20 dB above limit
MCPE	*(irrelevant)*	single freq.	3.93 dB	$P_{avg.}$ 30 dB above limit
MCPE	*(irrelevant)*	HT01	1.84 dB	$P_{avg.}$ at sensitivity limit
MCPE	*(irrelevant)*	HT01	1.87 dB	$P_{avg.}$ 10 dB above limit
MCPE	*(irrelevant)*	HT01	2.16 dB	$P_{avg.}$ 20 dB above limit
MCPE	*(irrelevant)*	HT01	4.03 dB	$P_{avg.}$ 30 dB above limit

Overall, the MCPE method (in particular in its original variant) is less favorable due to the significantly larger measurement uncertainty than the modified one or the TIS or AFS method.

7. Conclusions

An introduction to RCs and IOLW was given, and a reliability estimation of IOLW to determine necessary orders of magnitudes for sensitivity testing was presented. TIS, AFS and MCPE are proposed and evaluated in various variants to assess the OTA performance of an IOLW W-Device prototype.

The TIS method provides very good agreement with conducted measurements if single frequencies are used at a time and the antenna efficiency is considered. The MCPE method is related to the natural prospective operation of IOLW. However, the prospective low limit value for the PEP requires a large number of packets to be tested which is time consuming. Furthermore, the method is sensitive to outliers. Generally, the use of frequency hopping is more practical than the use of only one frequency at a time and saves measurement time. Methods or variants with continuous operation of the mode stirrers (i.e., AFS or modified MCPE) are significantly faster to perform than with stepped mode operation. However, outages sometimes make it difficult to interpret the measurements. These methods are suitable for relative measurements during development. Overall, the TIS method, for which there is also an essential correspondence in an AC, appears to be a suitable way to determine the OTA performance of IOLW products, particularly practical when using HT01.

However, there are some open tasks. In addition to a comprehensive measurement campaign to compare measurements of IOLW equipment obtained in different ACs and RCs, the test procedures and limit values have to be fixed in future and by the standardization working group. Furthermore, a comprehensive measurement uncertainty estimation shall be performed, and further tests regarding coexistence scenarios may be considered. Finally, the results shall be brought into the IEC standardization process of IOLW and its according test specification.

Author Contributions: Conceptualization, C.C.; methodology, C.C.; software, D.K. (Dmytro Krush) and D.K. (Dirk Krueger); formal analysis, C.C.; investigation, C.C.; data curation, C.C.; writing—original draft preparation, C.C.; writing—review and editing, D.K. (Dmytro Krush) and D.K. (Dirk Krueger) and C.C.; visualization, C.C.; supervision, G.S.; project administration, G.S. and C.C.; funding acquisition, G.S. All authors have read and agreed to the published version of the manuscript.

Funding: This research was funded by the Federal Ministry for Economic Affairs and Climate Action (BMWK, formerly: Federal Ministry for Economic Affairs and Energy (BMWi)) and the Project Management Jülich (PTJ) under the Wissens- und Technologietransfer durch Patente und Normen (WIPANO) program as project "IO-Link Wireless standardization for IEC-Approval (IOLW-4-IEC)", grant no. 03TN0005A and 03TN0005C. The APC was supported by the Open Access Fund of the Helmut-Schmidt-University, the University of the Federal Armed Forces Hamburg.

Institutional Review Board Statement: Not applicable.

Informed Consent Statement: Not applicable.

Data Availability Statement: Not applicable.

Acknowledgments: The authors thank H. Wattar, Kunbus GmbH, as well as R. Heynicke and T. Doebbert, Institute for Electrical Measurement Engineering, Helmut-Schmidt-University, for the fruitful discussions and continuous support.

Conflicts of Interest: The authors declare no conflict of interest.

Abbreviations

The following abbreviations are used in this manuscript:

AC	Anechoic chamber
AFS	Average fading sensitivity
BEP	Bit error probability
BLE	Bluetooth low energy
CBW	Coherence bandwidth
CDF	Cumulative distribution function
EIRP	Equivalent isotropic radiated power
EMC	Electromagnetic compatibility
EUT	Equipment under test
FA	Factory automation
F/TDMA	Frequency/time division multiple access
IEC	International Electrotechnical Commission
IFFT	Inverse fast Fourier transform
IIoT	Industrial Internet of Things
IOLW	IO-Link Wireless
ISM	Industrial, scientific and medical
MCPE	Mean channel packet error
MU	Measurement uncertainty
NLOS	Non line of sight
OCBW	Occupied channel bandwidth
OTA	Over-the-air
PDF	Probability density function
PDP	Power delay profile
PEP	Packet error probability
RC	Reverberation chamber
RF	Radio frequency
RFP	Residual failure probability
RSSI	Received signal strength indication
SISO	Single input single output
TIS	Total isotropic sensitivity
VNA	Vector network analyzer

References

1. Frotzscher, A.; Wetzker, U.; Bauer, M.; Rentschler, M.; Beyer, M.; Elspass, S.; Klessig, H. Requirements and current solutions of wireless communication in industrial automation. In Proceedings of the 2014 IEEE International Conference on Communications Workshops (ICC), Sydney, NSW, Australia, 10–14 June 2014; pp. 67–72. [CrossRef]
2. *IEC 61000-4-21:2011*; Electromagnetic Compatibility (EMC)—Part 4-21: Testing and Measurement Techniques—Reverberation Chamber Test Methods. International Electrotechnical Commission: Geneva, Switzerland, 2011.
3. Chen, X.; Zhu, S.; Zhang, A. Measurements of Antenna Systems in Reverberation Chamber: A Review. In Proceedings of the 2019 Cross Strait Quad-Regional Radio Science and Wireless Technology Conference (CSQRWC), Taiyuan, China, 18–21 July 2019; pp. 1–3. [CrossRef]

4. Cammin, C.; Krush, D.; Heynicke, R.; Scholl, G. Employing correlation for wireless components and device characterization in reverberation chambers. *J. Sens. Sens. Syst.* **2019**, *8*, 185–194. [CrossRef]
5. Yan, D.; Xu, Q.; Yu, C.; Huang, Y.; Loh, T.H. A Broadband Reference Antenna for Efficiency Measurements in a Reverberation Chamber. In Proceedings of the 2020 IEEE 3rd International Conference on Electronic Information and Communication Technology (ICEICT), Shenzhen, China, 13–15 November 2020; pp. 302–305. [CrossRef]
6. Holloway, C.L.; Hill, D.A.; Ladbury, J.M.; Wilson, P.F.; Koepke, G.; Coder, J. On the Use of Reverberation Chambers to Simulate a Rician Radio Environment for the Testing of Wireless Devices. *IEEE Trans. Antennas Propag.* **2006**, *54*, 3167–3177. [CrossRef]
7. Andersson, M.; Orlenius, C.; Kildal, P.S. Three Fast Ways of Measuring Receiver Sensitivity in a Reverberation Chamber. In Proceedings of the 2008 International Workshop on Antenna Technology: Small Antennas and Novel Metamaterials, Chiba, Japan, 4–6 March 2008; pp. 51–54. [CrossRef]
8. Horansky, R.D.; Remley, K.A. Flexibility in over-the-air testing of receiver sensitivity with reverberation chambers. *IET Microwaves Antennas Propag.* **2019**, *13*, 2590–2597. [CrossRef]
9. CTIA Certification. *Test Plan for Wireless Large-Form-Factor Device Over-the-Air Performance, Version Number 1.2.1*; CTIA Certification: Washington, DC, USA, 2020.
10. Primiani, V.M.; Barazzetta, M.; Bastianelli, L.; Micheli, D.; Moglie, E.; Diamanti, R.; Gradoni, G. Reverberation chambers for testing wireless devices and systems. *IEEE Electromagn. Compat. Mag.* **2020**, *9*, 45–55. [CrossRef]
11. Hubrechsen, A.; Remley, K.A.; Catteau, S. Reverberation Chamber Metrology for Wireless Internet of Things Devices: Flexibility in Form Factor, Rigor in Test. *IEEE Microw. Mag.* **2022**, *23*, 75–85. [CrossRef]
12. Genender, E.; Holloway, C.; Remley, K.; Ladbury, J.; Koepke, G.; Garbe, H. Use of reverberation chamber to simulate the power delay profile of a wireless environment. In Proceedings of the 2008 International Symposium on Electromagnetic Compatibility—EMC Europe, Hamburg, Germany, 8–12 September 2008; pp. 1–6. [CrossRef]
13. Kostas, J.; Boverie, B. Statistical model for a mode-stirred chamber. *IEEE Trans. Electromagn. Compat.* **1991**, *33*, 366–370. [CrossRef]
14. Rappaport, T.S. *Wireless Communications: Principles and Practice*, 2nd ed.; Prentice Hall: Upper Saddle River, NJ, USA, 2001.
15. Cammin, C.; Krush, D.; Heynicke, R.; Scholl, G. Test method for narrowband F/TDMA-based wireless sensor/actuator networks including radio channel emulation in severe multipath environments. *J. Sens. Sens. Syst.* **2018**, *7*, 183–192. [CrossRef]
16. Frolik, J. A case for considering hyper-Rayleigh fading channels. *IEEE Trans. Wirel. Commun.* **2007**, *6*, 1235–1239. [CrossRef]
17. Bastianelli, L.; Gradoni, G.; Micheli, D.; Barazzetta, M.; Diamanti, R.; Moglie, F.; Primiani, V.M. Reverberation chambers for testing LTE wireless communication systems. In Proceedings of the 2017 International Conference on Electromagnetics in Advanced Applications (ICEAA), Verona, Italy, 11–15 September 2017; pp. 722–725. [CrossRef]
18. Genender, E.; Holloway, C.L.; Remley, K.A.; Ladbury, J.M.; Koepke, G.; Garbe, H. Simulating the Multipath Channel With a Reverberation Chamber: Application to Bit Error Rate Measurements. *IEEE Trans. Electromagn. Compat.* **2010**, *52*, 766–777. [CrossRef]
19. Chen, X.; Kildal, P.S.; Orlenius, C.; Carlsson, J. Channel Sounding of Loaded Reverberation Chamber for Over-the-Air Testing of Wireless Devices: Coherence Bandwidth Versus Average Mode Bandwidth and Delay Spread. *IEEE Antennas Wirel. Propag. Lett.* **2009**, *8*, 678–681. [CrossRef]
20. Chen, X.; Kildal, P.S.; Orlenius, C.; Carlsson, J. Corrections to "Channel Sounding of Loaded Reverberation Chamber for Over-the-Air Testing of Wireless Devices—Coherence Bandwidth Versus Average Mode Bandwidth and Delay Spread". *IEEE Antennas Wirel. Propag. Lett.* **2013**, *12*, 1728. [CrossRef]
21. Kildal, P.S.; Chen, X.; Orlenius, C.; Franzen, M.; Patane, C.S.L. Characterization of Reverberation Chambers for OTA Measurements of Wireless Devices: Physical Formulations of Channel Matrix and New Uncertainty Formula. *IEEE Trans. Antennas Propag.* **2012**, *60*, 3875–3891. [CrossRef]
22. Hubrechsen, A.; Remley, K.A.; Jones, R.D.; Horansky, R.D.; Neylon, V.T.; Bronckers, L.A. NB-IoT devices in reverberation chambers: A comprehensive uncertainty analysis. *Int. J. Microw. Wirel. Technol.* **2021**, *13*, 561–568. [CrossRef] [PubMed]
23. *VDI/VDE 2185*; Radio Based Communication in Industrial Automation. German Association for Electrical, Electronic and Information Technologies: Düsseldorf, Germany, 2009.
24. IO-Link Community. IO-Link Wireless System Extensions—Specification Version 1.1. March 2018, Order No: 10.112. 2018. Available online: https://io-link.com/share/Downloads/System-Extensions/IO-Link_Wireless_System_10112_V11_Mar18.pdf (accessed on 11 January 2022).
25. IO-Link Community. IO-Link Wireless System Extensions—Specification V1.1.3 June 2022, Order No: 10.112. 2022. Available online: https://io-link.com/share/Downloads/System-Extensions/IOLW-Spec_10112_V113_Jun22.pdf (accessed on 11 July 2022).
26. IO-Link Community. IO-Link Interface and System Specification Version 1.1.3, June 2019, Order No: 10.032. 2019. Available online: https://io-link.com/share/Downloads/Package-2020/IOL-Interface-Spec_10002_V113_Jun19.pdf (accessed on 22 April 2022).
27. *IEC 61131-9:2022*; Programmable Controllers—Part 9: Single-Drop Digital Communication Interface for Small Sensors and Actuators (SDCI). International Electrotechnical Commission: Geneva, Switzerland, 2022.
28. Heynicke, R.; Krush, D.; Cammin, C.; Scholl, G.; Kaercher, B.; Ritter, J.; Gaggero, P.; Rentschler, M. IO-Link Wireless enhanced factory automation communication for Industry 4.0 applications. *J. Sens. Sens. Syst.* **2018**, *7*, 131–142. [CrossRef]
29. Doebbert, T.R.; Cammin, C.; Scholl, G. Safety Architecture Proposal for Low-Latency Sensor/Actuator Networks using IO-Link Wireless. *IEEE Access* **2022**, *10*, 3030–3044. [CrossRef]

30. IEC 61139-3 ED1 (Project). Industrial Networks—Single-Drop Digital Communication Interface—Part 3: Wireless Extensions. 2022. Available online: https://www.iec.ch/ords/f?p=103:38:1857208095061::::FSP_ORG_ID,FSP_APEX_PAGE,FSP_PROJECT_ID:1376,20,104747 (accessed on 10 July 2022).
31. Krush, D.; Cammin, C.; Doebbert, T.R.; Heynicke, R.; Scholl, G. Coexistence Management Methods and Tools for IO-Link Wireless. In Proceedings of the 2021 17th IEEE International Conference on Factory Communication Systems (WFCS), Linz, Austria, 9–11 June 2021; pp. 151–158. [CrossRef]
32. Wolberg, D.; Rentschler, M.; Gaggero, P. Simulative performance analysis of IO-link wireless. In Proceedings of the 2018 14th IEEE International Workshop on Factory Communication Systems (WFCS), Imperia, Italy, 13–15 June 2018; pp. 1–10. [CrossRef]
33. ICAO. BER Estimation through Packet Error Rate Measurement. 2014. Available online: https://www.icao.int/safety/acp/ACPWGF/ACP-WG-S-Web%20Meeting%205/ACP-WG-S_WP04-ErrorMeasurment_r11%20%20(2).docx (accessed on 6 April 2022).
34. Luo, J.; Mendivil, E.; Christopher, M. Obtaining total isotropic sensitivity from average fading sensitivity in reverberation chamber. In Proceedings of the 2017 IEEE International Symposium on Antennas and Propagation USNC/URSI National Radio Science Meeting, San Diego, CA, USA, 9–14 July 2017; pp. 241–242. [CrossRef]
35. Friis, H. A Note on a Simple Transmission Formula. *Proc. IRE* **1946**, *34*, 254–256. [CrossRef]
36. Rappaport, T.S. Indoor radio communications for factories of the future. *IEEE Commun. Mag.* **1989**, *27*, 15–24. [CrossRef]
37. *ITU—Recommendation ITU-R P.1238-10 (08/2019)*; Propagation Data and Prediction Methods for the Planning of Indoor Radiocommunication Systems and Radio Local Area Networks in the Frequency Range 300 MHz to 450 GHz. ITU: Geneva, Switzerland, 2019.
38. *ETSI EN 300 328 V2.2.2 (2019-07)*; Wideband Transmission Systems; Data Transmission Equipment Operating in the 2,4 GHz Band; Harmonized Standard for Access to Radio Spectrum. ETSI: Sophia Antipolis, France, 2019.
39. Cammin, C.; Krush, D.; Heynicke, R.; Scholl, G. Sensing Reverberation Chamber Loading for IO-Link Wireless Testing. In Proceedings of the 2021 International Conference on Electromagnetics in Advanced Applications (ICEAA), Honolulu, HI, USA, 9–13 August 2021; pp. 087–091. [CrossRef]
40. Remley, K.A.; Dortmans, J.; Weldon, C.; Horansky, R.D.; Meurs, T.B.; Wang, C.M.; Williams, D.F.; Holloway, C.L.; Wilson, P.F. Configuring and Verifying Reverberation Chambers for Testing Cellular Wireless Devices. *IEEE Trans. Electromagn. Compat.* **2016**, *58*, 661–672. [CrossRef]
41. Xue, W.; Li, F.; Chen, X. Effects of Signal Bandwidth on Total Isotropic Sensitivity Measurements in Reverberation Chamber. *IEEE Trans. Instrum. Meas.* **2021**, *70*, 1–8. [CrossRef]
42. *3GPP TR 25.914 V16.0.0 (2020-07)*; Measurements of Radio Performances for UMTS Terminals in Speech Mode. 3GPP: Sophia-Antipolis, France, 2020.
43. Luo, J.; Mendivil, E.; Christopher, M. Over-the-Air Performance Evaluation of NB-IoT in Reverberation Chamber and Anechoic Chamber. In Proceedings of the 2018 AMTA Proceedings, Williamsburg, VA, USA, 4–9 November 2018; pp. 1–3.
44. Orlenius, C.; Kildal, P.S.; Poilasne, G. Measurements of total isotropic sensitivity and average fading sensitivity of CDMA phones in reverberation chamber. In Proceedings of the 2005 IEEE Antennas and Propagation Society International Symposium, Washington, DC, USA, 3–8 July 2005; Volume 1A, pp. 409–412. [CrossRef]
45. Shen, P.; Qi, Y.; Yu, W.; Li, F.; Fan, J. Fast and Accurate TIS Testing Method for Wireless User Equipment With RSS Reporting. *IEEE Trans. Electromagn. Compat.* **2016**, *58*, 887–895. [CrossRef]
46. Senic, D.; Cavaliere, D.; North, M.V.; Becker, M.G.; Remley, K.A.; Wang, C.M.; Holloway, C.L. Isotropy study for over-the-Air measurements in a loaded reverberation chamber. In Proceedings of the 2017 IEEE International Symposium on Electromagnetic Compatibility Signal/Power Integrity (EMCSI), Washington, DC, USA, 7–11 August 2017; pp. 124–129. [CrossRef]
47. Horansky, R.D.; Meurs, T.B.; North, M.V.; Wang, C.M.; Becker, M.G.; Remley, K.A. Statistical Considerations for Total Isotropic Sensitivity of Wireless Devices Measured in Reverberation Chambers. In Proceedings of the 2018 International Symposium on Electromagnetic Compatibility (EMC EUROPE), Amsterdam, The Netherlands, 27–30 August 2018; pp. 398–403. [CrossRef]
48. Coder, J.B.; Ladbury, J.M.; Holloway, C.L.; Remley, K.A. Examining the true effectiveness of loading a reverberation chamber: How to get your chamber consistently loaded. In Proceedings of the 2010 IEEE International Symposium on Electromagnetic Compatibility, Fort Lauderdale, FL, USA, 25–30 July 2010; pp. 530–535. [CrossRef]
49. Chen, X.; Kildal, P.S.; Lai, S.H. Estimation of Average Rician K-Factor and Average Mode Bandwidth in Loaded Reverberation Chamber. *IEEE Antennas Wirel. Propag. Lett.* **2011**, *10*, 1437–1440. [CrossRef]
50. Bastianelli, L.; Giacometti, L.; Primiani, V.M.; Moglie, F. Effect of absorber number and positioning on the power delay profile of a reverberation chamber. In Proceedings of the 2015 IEEE International Symposium on Electromagnetic Compatibility (EMC), Dresden, Germany, 16–22 August 2015; pp. 422–427. [CrossRef]
51. Hubrechsen, A.; Neylon, V.T.; Remley, K.A.; Jones, R.D.; Horansky, R.D.; Bronckers, L.A. A Preliminary Study on Uncertainty of NB-IoT Measurements in Reverberation Chambers. In Proceedings of the 2020 50th European Microwave Conference (EuMC), Utrecht, The Netherlands, 12–14 January 2021; pp. 1051–1054. [CrossRef]
52. Bluetest AB. RTS60 Reverberation Test System—Datasheet Rev. G. Available online: https://bluetest.se/files/RTS60_BTD-10-019_Rev_G.pdf (accessed on 20 Macrh 2022).
53. DVTEST. dbSAFE RME (Leaflet). Available online: https://www.dvtest.com/pub/media/sparsh/product_attachment/dbSAFE_RME_Final_2021_compressed.pdf (accessed on 20 Macrh 2022).

54. DVTEST. dbSAFE RME Datasheet. Available online: https://dvtest.com/pub/media/sparsh/product_attachment/DVTEST_dbSAFE_RME_Datasheet.pdf (accessed on 20 Macrh 2022).
55. Cammin, C.; Krush, D.; Heynicke, R.; Scholl, G. Deep Fading in a Reverberation Chamber for Wireless Device Testing. *IOP Conf. Ser. Mater. Sci. Eng.* **2020**, *766*, 012004. [CrossRef]
56. CTIA Certification. *CTIA Certification Test Plan for Wireless Device Over-the-Air Performance, Version Number 3.9.4.*; CTIA Certification: Washington, DC, USA, 2020.
57. *JCGM 100:2008*; Evaluation of Measurement Data—Guide to the Expression of Uncertainty in Measurement (GUM). Joint Committee for Guides in Metrology (JCGM)—BIPM: Sèvres Cedex, France, 2008.